Applications of wavepacket methodology

By A. Stolow

Steacie Institute for Molecular Sciences,
National Research Council of Canada, Ottawa,
Ontario, Canada K1A 0R6

Wavepackets, coherent sums of quantum states, are now well understood both theoretically and experimentally in terms of their creation, evolution and detection. When mature enough, wavepacket methods might themselves be considered a 'technology'. In this paper we address this conjecture and consider the application of wavepacket ideas and techniques to problems such as coherent control, lifetimes of Rydberg states and laser isotope separation. We suggest that wavepacket methods might be thought of more broadly as a potential tool to solve a variety of practical problems.

**Keywords: wavepacket revivals; femtosecond dynamics; coherent control;
Rydberg states; isotope separation; wavepacket interferometry**

1. Introduction

Wavepackets are coherent sums of quantum states created by short phase-controlled optical pulses. The free evolution of wavepackets is determined by the dynamics of the system and, consequently, wavepacket methods are used to study fast atomic (for example, Nauenberg *et al.* 1994), molecular (for example, Zewail 1994; Manz & Wöste 1995) and condensed phase (for example, Barbara *et al.* 1994) processes. They can be used to prepare zero-order states, allowing us to observe their classical-like behaviour and gain physical insight into the dynamics of the system. They can be used for spectroscopy in the time domain and can be complementary to high-resolution spectroscopy, especially in cases where there are broad ranges of excited state lifetimes. Wavepackets have gained prominence as a method for the quantum control (Tannor & Rice 1988) of dynamical processes such as photodissociation or ionization. The control of wavepacket dynamics through the shaping of ultrashort laser pulses (Shi *et al.* 1988; Pierce *et al.* 1990; Kosloff *et al.* 1989; Yan *et al.* 1993; Krause *et al.* 1995; Wefers *et al.* 1995; Melinger *et al.* 1994; Kohler *et al.* 1995; Bardeen *et al.* 1995; Schumacher *et al.* 1995) is a major area of investigation.

Wavepacket ideas, techniques and methods of analysis are quite well understood, both experimentally and theoretically. As these wavepacket methods mature, we ponder the question: could wavepacket methods be considered as a general and flexible 'technology' to be applied to a variety of practical problems? In this paper, we address this question by considering various examples of the application of wavepackets. We describe wavepacket phenomenology and give a typical example. We compare wavepacket methods with coherent phase control methods and show that they can be thought of as the same physics. From this point of view, there are many successful demonstrations of coherent control. We go on to discuss wavepackets applied to

TEX Paper

problems in ion–Rydberg collisions, Rydberg lifetime enhancement, isotope separation and ultrafast switching, all of which address our general question about the use of wavepackets as a tool.

2. Wavepacket phenomenology

In this section we review typical wavepacket behaviour and introduce concepts to be used in following sections. There are three aspects to a wavepacket experiment: the preparation, the evolution and the detection. The preparation (pump) pulse coherently excites a superposition of excited state levels—a wavepacket. The amplitudes and initial phases of these prepared states are determined by the initial ground state population, the pump laser and the transition amplitudes. Once the pump laser pulse is over the wavepacket, given by equation (2.1), evolves freely according to relative energy phase factors in the superposition,

$$|\chi(\Delta t)\rangle = \sum_n a_n |\nu_n\rangle e^{-i2\pi c E_n(\nu_n)\Delta t}. \tag{2.1}$$

The a_n coefficients contain both the amplitudes and initial phases of the states $|\nu_n\rangle$ which are prepared by the pump laser. The E_n are the excited state term values in wavenumbers.

The probe laser pulse interacts with the wavepacket after the pump pulse is over, at some time delay Δt. The final detection step is usually incoherent because the measured signal is a sum of the final state populations . Therefore, the time dependence of the signal $S(\Delta t)$ can be visualized in terms the following equation:

$$S(\Delta t) = \sum_n \sum_m b_n b_m \cos(E_n - E_m)2\pi c \Delta t. \tag{2.2}$$

For the case of vibrational wavepackets, the b_n coefficients contain the a_n as well as the transition dipole moment and Franck–Condon factors to the final state. The measured signal, $S(\Delta t)$ is related to the overlap of the coherent sum of prepared states with a given final state and is modulated as a function of time. The modulations are due to interferences between the individual transitions from different eigenstates terminating in the same final state and are described by nearest-neighbour coherences (i.e. when $n = m \pm 1$) as well as higher-order coherences (e.g. next nearest neighbour, $n = m \pm 2$).

Vibrational wavepackets in the bound electronic B state of iodine, studied by Zewail (for example, Dantus *et al.* 1991; Gruebele & Zewail 1993), show some typical wavepacket phenomena. Wavepacket studies have been performed by Gerber on the bound electronic states of the Na_2 (for example, Baumert *et al.* 1992) system. Other bound state studies have included the Li_2 (Williams *et al.* 1996), K_2 (de Vivie Riedle *et al.* 1996) and Cs_2 (Blanchet *et al.* 1995; Rodriguez *et al.* 1995) molecules. Wavepacket phenomena on coupled (predissociative) electronic states have been observed for the molecules NaI (Rose *et al.* 1988*a*,*b*, 1989) and IBr (Vrakking *et al.* 1996*a*). We show an example of typical wavepacket evolution (figure 1, top) in the I_2 B state, as observed using ionization detection (Fischer *et al.* 1995). For a pump pulse around 580 nm, a set of vibrational levels around $v' = 15$ is prepared. The level spacing around $v' = 15$ leads to modulations with a period of 340 fs (i.e. the average classical vibrational period of $I_2(B)$ around $v' = 15$ is 340 fs). Since the level spacings vary due to the anharmonicity of the B state potential, as time goes on, the
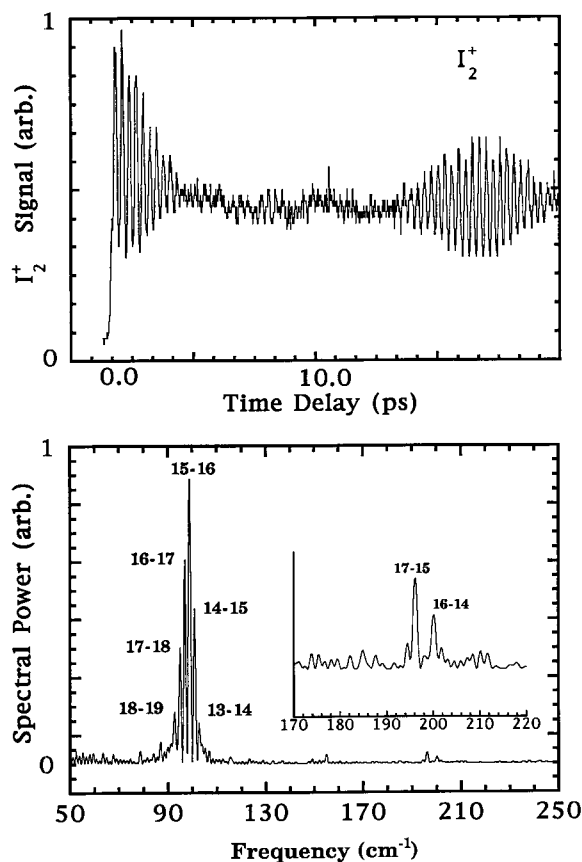
Figure 1. (Top) Example of typical wavepacket phenomena: coherent oscillation, dephasing due to anharmonicities and subsequent revival (in the vibrational system iodine B state). (Bottom) Fourier transform power spectrum of the above time domain data, showing that all frequencies observed can be assigned to interferences between nearest- (near 100 cm^{-1}) and next-nearest- (near 200 cm^{-1}) neighbour transitions.

340 fs modulations disappear by about 5 ps as the vibrational states get out of phase with each other. The phase relationships between the states remain well defined, and therefore the states rephase, giving rise to a recurrence near 18 ps (called the half revival) where the 340 fs modulation is seen again. It was shown (Averbukh & Perel'man 1991) that groups of strongly localized wavepackets appear around times $t \approx (p/q)T_{\text{rev}}$, where p/q is an irreducible fraction of integers. For example, around time $t \approx \frac{1}{2}T_{\text{rev}}$, the half revival, the first recurrence of the wavepacket to its original shape takes place. The effects of dephasing only manifest themselves in a $180°$ phase shift of the wavepacket motion with respect to the initial motion. Around time $t \approx T_{\text{rev}}$, the full revival, the wavepacket revives without any phase shift and appears exactly as the initial wavepacket. For $q > 2$, fractional revivals of the original wavepacket occur where the wavepacket splits into a number of smaller subwavepackets. For example, at the quarter revivals (i.e. when $p/q = \frac{1}{4}$), the wavepacket splits into two equal parts exactly out of phase, leading, at these characteristic times, to a doubling of the modulation frequency in the time delay scan (Vrakking *et al.* 1996*b*). We note that revivals of wavepackets have been observed both in atomic (Yeazell *et al.* 1990; Yeazel & Stroud 1991; Meacher *et al.* 1991; Wals *et al.* 1994; Marmet *et al.*
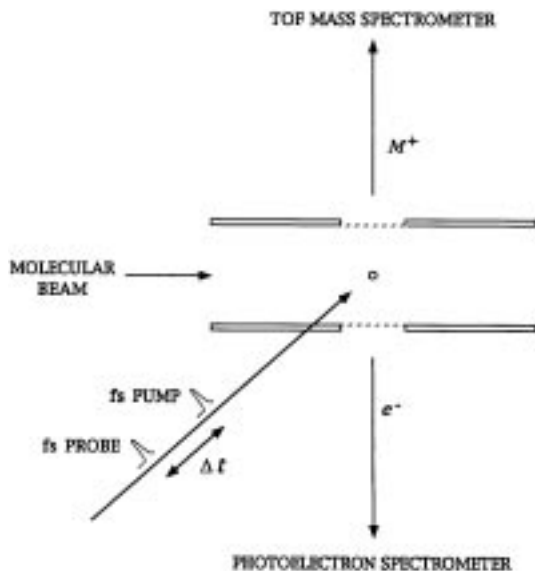
Figure 2. Typical wavepacket experiment. Wavepackets in atoms or molecules, introduced by a molecular beam, are prepared by the pump pulse. After a free evolution time Δt, the wavepackets are interrogated by the probe laser pulse. In the case shown, the measured signal is an ion and/or photoelectron signal.

1994) and molecular systems (Fischer *et al.* 1995; Gruebele *et al.* 1990; Baumert *et al.* 1992).

A discrete Fourier transform power spectrum of the data from figure 1 (top) are shown in figure 1 (bottom), revealing the spectral content of the time domain data. The largest peak, centred around $\omega = 99 \, \mathrm{cm}^{-1}$, can be assigned to the level spacing between $v' = 15$ and $v' = 16$ in the B state. The other peaks are assigned to other first-order coherences as indicated. It can be seen that the second-order coherences (inset), near $200 \, \mathrm{cm}^{-1}$, have twice the spacing of the first-order coherences, as expected from the level structure. The above is an example of typical wavepacket behaviour.

3. Experimental

In our experiments, a phase-lock synchronized amplified femtosecond Ti:sapphire/picosecond Nd:YAG laser (Villeneuve *et al.* 1995) is used as the pump source for this amplification. Broad tunability is required and was achieved by generating a white light continuum and re-amplifying the desired colour. A molecular beam photoelectron/photoion spectrometer was used to produce pulsed supersonic molecular beams. The femtosecond pump and probe lasers intersected the beam at the interaction point of the spectrometer, depicted in figure 2, and both ion and photoelectron signals can be recorded as a function of time delay, as described in detail elsewhere (Fischer *et al.* 1996).

4. Coherent control and wavepacket experiments

In a wavepacket experiment, as discussed above, the modulations in the observed signal are due to interferences between the individual transitions from different eigen-
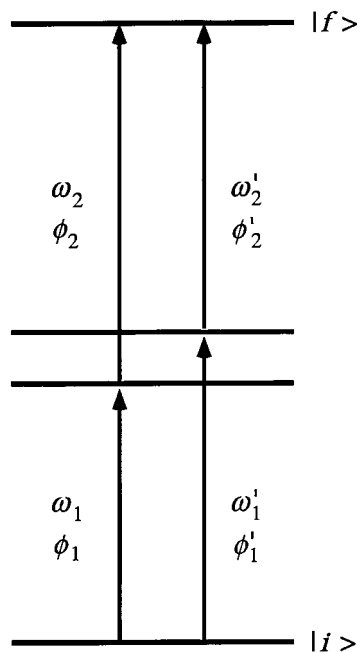
Figure 3. Coherent phase control scheme based upon well-resolved two-photon transitions (a $2/2'$ scheme). The requirements for final state population control are: (i) energy degeneracy $(\omega_1 + \omega_2) = (\omega'_1 + \omega'_2)$; (ii) optical control over the relative phase constant between paths 2 and $2'$, $(\phi_1 + \phi_2) - (\phi'_1 + \phi'_2) = \text{const}$.

states terminating in the same final state. This is very similar to the requirements of coherent phase control, a subject of great recent interest (Brumer & Shapiro 1989, 1992), where final state control is achieved through the quantum mechanical interference of two distinct yet degenerate pathways. In figure 3, we show one example of a coherent control scenario, here based upon the interference of two-photon transitions (the so-called $2/2'$ scheme). The inital state $|i\rangle$ is excited to the target state $|f\rangle$ via a two-photon transition with photons ω_1 and ω_2, through a resonant intermediate state (bound or continuum). This same $|i\rangle$ state is simultaneously excited to $|f\rangle$ through another two-photon transition with photons ω'_1 and ω'_2. The optical phases of the fields are labelled ϕ_1, ϕ_2, ϕ'_1 and ϕ'_2, respectively. The first necessary condition for coherent control is energy degeneracy:

$$\omega_1 + \omega_2 = \omega'_1 + \omega'_2. \tag{4.1}$$

The second necessary condition is for control over the optical phase difference between the two paths:

$$(\phi_1 + \phi_2) - (\phi'_1 + \phi'_2) = p_0. \tag{4.2}$$

The p_0 in equation (4.2) is the variable used to achieve constructive or destructive interference in the final state $|f\rangle$. The pairs (ω_1, ω'_1) must be phase locked and the same is true for the (ω_2, ω'_2) fields. However, the pairs (ω_1, ω_2) and (ω'_1, ω'_2) need not be phase locked since the total phase $(\phi_1 + \phi_2) + (\phi'_1 + \phi'_2)$ is abritrary. Typically, phase variation between the paths is achieved by passing one control path, e.g. (ω_1, ω_2), through a gas cell with variable pressure and hence refractive index and, therefore, varying the phase delay between the two paths (Park *et al.* 1991; Wang *et al.* 1996).
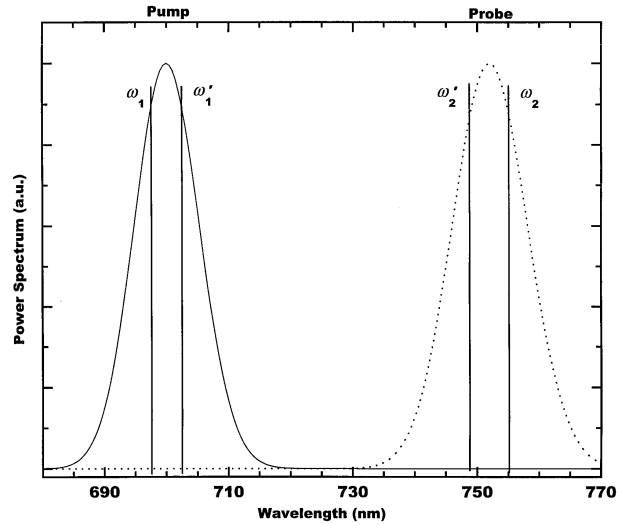
Figure 4. Femtosecond pulses by definition have phase control over the broad range of frequencies comprising the pulse. One way to achieve the requisite phased pairs of frequencies (ω_1, ω_1') and (ω_2, ω_2'), is to filter them out of femtosecond pulses containing these frequencies. If filters are not used, this experiment is commonly described as a femtosecond pump-probe measurement.

For the sake of this discussion, we assume that the probability of being in the target state $|f\rangle$ is maximal when there is a π phase shift between these two transitions.

A simple way to obtain phase locked pairs of fields (ω_1, ω_1') and (ω_2, ω_2') is to filter them out of a transform-limited short pulse, as shown in figure 4. By definition, a short pulse is composed of a broad range of phase locked frequencies. One pulse contains the frequencies ω_1 and ω_1' and another pulse contains the frequencies ω_2 and ω_2'. The vertical lines in figure 4 indicate the narrow linewidth filters used to select the desired frequencies.

A simple way to vary the optical phase between the two paths is to introduce a time delay Δt, as shown in figure 5, between the two broad bandwidth pulses (the solid line represents the pulse containing ω_1 and ω_1'; the dotted line represents the pulse containing ω_2 and ω_2'). As can be seen in equation (4.3), adding Δt to a pulse delay merely adds a frequency dependent phase shift to all the frequencies comprising the pulse,

$$\exp\{-i[\omega t + \phi_0]\} \Rightarrow \exp\{-i[\omega(t + \Delta t) + \phi_0]\}$$
$$= \exp\{-i[\omega t + \omega\Delta t + \phi_0]\} = \exp\{-i[\omega t + (\phi_1 + \phi_0)]\}, \quad (4.3)$$

where

$$\phi_1 = \omega\Delta t. \tag{4.4}$$

If we delay the second broad band pulse by Δt, we introduce a phase shift of both ω_2 and ω_2'. However, the phases of these two frequencies do not change at the same rate since time delay is by definition a frequency dependent phase shift (equation (4.4)). Therefore, since the total phase is arbitrary, delaying the second pulse just introduces a relative phase shift between ω_2 and ω_2'; this is the control required, as indicated by equation (4.2). Based upon our assumption above, we expect that when the phase shift between the transitions is π, the formation of the target state is maximized.

It is interesting to note that if we removed the frequency filters shown in figure 4, we would describe this as a femtosecond pump-probe measurement of the
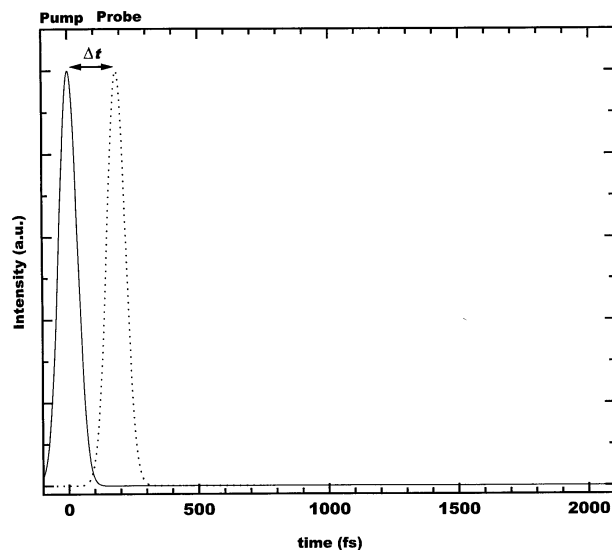
Figure 5. Using the scheme of figure 4 to select phased pairs of frequencies, the relative phase between the paths 2 and 2′ may be varied by delaying the pulse containing (ω_1, ω_1') with respect to the pulse containing (ω_2, ω_2'). As phase is by definition a frequency-dependent time delay, changing Δt changes simultaneously the total phases of paths 2 and 2′, but at different rates. This amounts to relative control over the phases between the paths. As the filters in figure 4 are removed, the isomorphism of coherent control with femtosecond pump-probe experiments may be seen.

intermediate state dynamics. The eigensystem shown in figure 3 will itself, through resonance, select the pairs of frequencies (ω_1, ω_1') and (ω_2, ω_2'). Upon varying Δt, the two intermediate states will alternate (on the timescale determined by the level splitting) between constructive and destructive interference in the final state $|f\rangle$. As discussed in §1, since a femtosecond pump-probe experiment is based upon interferences between degenerate transitions, we can see it is the same as a 2/2′ control scenario.

We now consider coming at this problem from the femtosecond pump-probe point of view. A typical femtosecond pump-probe experiment prepares a wavepacket on intermediate states of the eigensystem of figure 3. The wavepacket will be π out of phase with respect to the initial wavepacket at a characteristic time T, determined by the level spacing. At this time, based upon our phase assumption, the wavepacket would overlap favourably with the final state. In the language of pump-probe experiments, we detect the wavepacket motion by monitoring the signal to the final state. At $2T$, the excited state wavepacket will be exactly reconstructed. If we wished to multiplex our experiment, we would repeat the femtosecond pump-probe measurement when the wavepacket has returned to its initial condition: we repeat the experiment every $2T$, as is shown in figure 6, each time optimally transferring the signal to $|f\rangle$.

The Fourier transform power spectra of the pulse trains in figure 6 are shown in figure 7. We can see that this repetitive pump-probe scheme creates exactly the sharp pairs of frequencies (ω_1, ω_1') and (ω_2, ω_2') required for the 2/2′ control scenario shown in figure 3. Again, we can see the equivalence of the 2/2′ scenario with femtosecond pump-probe measurements.

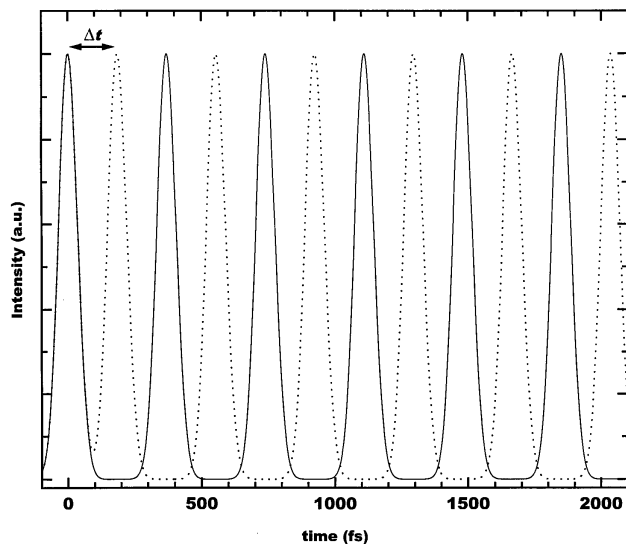The point of this discussion is to illustrate that femtosecond experiments can be

Figure 6. A typical femtosecond pump-probe experiment, using the unfiltered pulses from figure 5, may be repeated periodically, each time the system returns to the initial condition after a time $2\Delta t$.
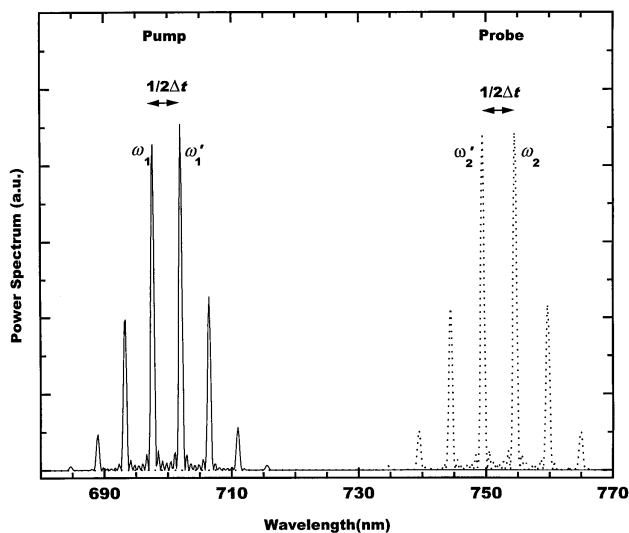

Figure 7. Fourier transform power spectra of the pulse trains shown in figure 6. It can be seen that as time evolves, the spectra of the pump and probe lasers evolve into the sharp frequencies $\omega_1, \omega_1', \omega_2, \omega_2'$. These are exactly the frequencies required for the control control scheme described in figure 4, again showing the isomorphism between these methods.

thought of as coherent control experiments and have given many successful examples (for example, Zewail 1994; Manz & Wöste 1995) of robust final state control. This is quite encouraging. Coherent oscillations in femtosecond experiments have been observed in very large biological systems (Wang *et al.* 1994) and in solution (Pugliano *et al.* 1993; Banin *et al.* 1992), suggesting, in fact, that coherent control is very broadly applicable and that wavepacket methods are indeed a good tool for this control.

5. Microsecond effects studied with wavepackets

Wavepacket techniques are usually thought of as being sensitive to very fast processes. In this example, we show that appropriate wavepacket methods can in fact be developed to probe effects which happen on much long timescales (here, microseconds).

Zero kinetic energy photoelectron spectroscopy (ZEKE) is a molecular photoelectron spectroscopy technique developed to provide a high sensitivity method with rotational resolution (Müller-Dethlefs *et al.* 1984; Müller-Dethlefs & Schlag 1991). The technique is based upon delayed pulsed field ionization of long-lived high-lying ($n = 100$–200) molecular Rydberg states. The lifetimes of these high-n Rydberg states are actually much longer than expected because they are enhanced by changes to the angular momentum quantum numbers l and m of the Rydberg electron (Chupka 1993). The changes to l can arise from DC electric fields in the apparatus which spoil spherical symmetry. Since the decay rate of Rydberg states is determined by close-range interactions with the core, their lifetime is relatively short for low l and becomes very long for high l (Vrakking & Lee 1995). A further effect is suggested to be due to nearby ions which change both l and m, spoiled by both spherical and cylindrical asymmetry (Merkt & Zare 1995), giving an expected further lifetime enhancement. Ion–Rydberg interactions might therefore cause incoherent 'diffusion' of Rydberg population over all l and m, leading to a long lifetimes. In the following, we show that wavepacket methods can be used to observe these ion–Rydberg interactions which enhance the lifetimes of molecular Rydberg states on the microsecond timescale.

In figure 8 (top), we show the results of a vibrational wavepacket experiment on I_2 B state, identical to that shown in figure 1 except using ZEKE (i.e. delayed pulsed field ionization using electron detection), rather than ion detection. An interesting difference between the ZEKE (figure 8) and ion scans (figure 1) is the modulation depths. They are much deeper in the ZEKE signals. These difference are only due to differences between the ion and ZEKE detection mechanisms. Furthermore, we note that in the power spectra shown in figure 1 (bottom) and figure 8 (bottom), the second harmonic contribution is very small in the ion scans, but much more prominent in the ZEKE scan. In the latter there are peaks near $200\,\mathrm{cm}^{-1}$, labelled by an asterisk in figure 8 that are not assignable to next-nearest-neighbour coherences and in fact do not correspond to any level spacings in the isolated molecule. Therefore, they cannot come from isolated molecules. In fact, the peaks labelled by an asterisk are assignable to *sum frequencies* of nearest-neighbour coherences. There is a nonlinear mixing of the Fourier components in the ZEKE detection scheme and not in the ion detection scheme.

The Rydberg states prepared by the laser are low-l states which have significant overlap with the ion core (hence, a non-zero decay rate). The n states which survive (long enough to detect after $1\,\mu\mathrm{s}$) will have high-l character. We can understand the stabilization to originate from (l, m)-changing interactions of a Rydberg state with an ion. This implies that there is a coupling of Rydberg state lifetime to ion concentration. In this experiment, the ion signal and, hence, concentration is modulated by the wavepacket motion. The same is true for the *preparation* of Rydberg states. However, it is insufficient to just prepare Rydberg states: they must be *detected* after the microsecond delay time and this requires an interaction with ions in order to increase l. This implies that the ion concentration modulates again the Rydberg *detection*
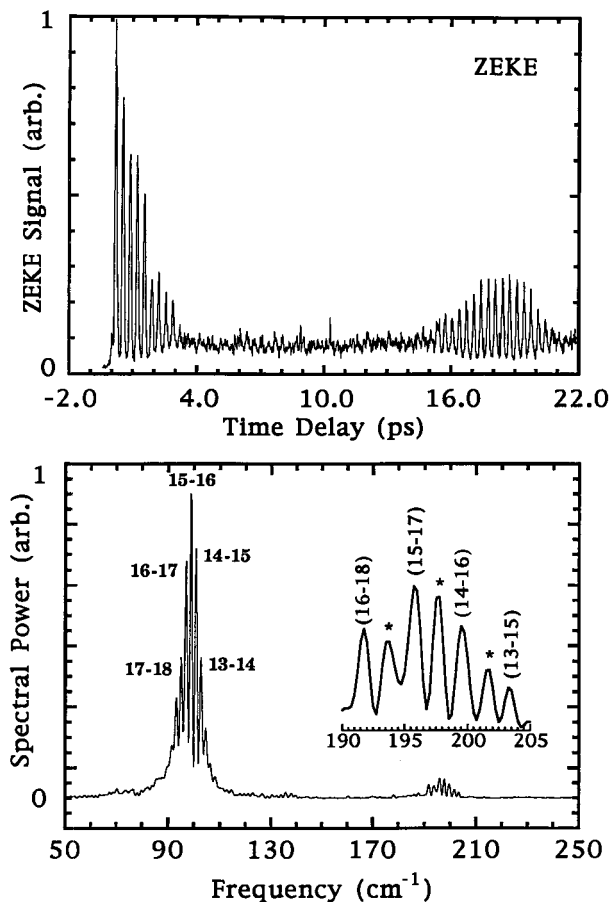
Figure 8. Use of wavepacket methods in the study of phenomena on long timescales, here show-ing the effect of ion–Rydberg interactions over the microsecond lifetimes of high-n Rydberg states. ZEKE detection of I_2 B state wavepacket dynamics (top) . The wavepacket evolution modulates both ion and Rydberg state concentration. The microsecond timescale interaction leads to a double modulation, appearing as 'forbidden' lines marked with an asterisk in the Fourier transform power spectrum (bottom). For a discussion, see the text.

efficiency. The ZEKE signal is a double modulation: it is a product of the proba-bility of preparation times the probability of detection. Both factors behave as the ion concentration. This leads to the cross-terms in the observed ZEKE modulation frequencies and to enhanced modulation depths. Although the double modulation occurs at short times, the effects of it are not discernible until microsecond timescales are achieved. This argument, along with further supporting evidence and theoretical modelling, is discussed in detail in a separate publication (Vrakking *et al.* 1995).

The above provides an unusual example of wavepacket methods applied to a prob-lem in another field and illustrates how femtosecond techniques can be used to char-acterize phenomena occuring on much longer timescales.

6. Nanosecond wavepackets using electric and magnetic fields

In conventional ZEKE experiments with 'incoherent' nanosecond lasers, Rydberg electronic wavepackets are in fact always prepared due to the fact that the inverse

density of states at Rydberg high-n is much less than the narrow coherent bandwidths of these laser pulses. What are the potential consequences of this recognition? Wavepacket methods and ways of thinking can be used on longer timescales to control processes using applied external fields (here, electric and magnetic), rather than the usual optical fields. In this example, we can enhance the lifetimes of high-lying Rydberg states without the use of external ions, as in the previous section. This particular scheme makes use of pulsed crossed electric and magnetic fields and can also be thought of an extension of coherent control ideas to beyond the optical domain.

The idea of wavepacket lifetime enhancement is that a pulsed electric field is applied during the Rydberg preparation, leading to revival structure in a Stark wavepacket (Wals *et al.* 1994). In terms of angular momentum states, this wavepacket evolves periodically from the initially prepared low-l to the high-l states. After a full period, the Stark wavepacket has returned to the initial low-l state prepared by the laser. At the half period, the Stark wavepacket has achieved its maximal angular momentum. Therefore, we turn off the electric field at the half period, leaving the wavepacket at high l. The high-l states should be long lived. Due to the presence of stray electric fields (mV cm^{-1}) and core multipoles, however, this state will not be stable (Bixon & Jortner 1996; Remacle & Levine 1996; Baranov *et al.* 1996) (i.e. it will *eventually* return to low l). We therefore apply a crossed magnetic field pulse exactly when the wavepacket is in high-l states, causing a coherent periodic evolution in the Zeeman states. This m wavepacket is initially at low m and evolves towards high m according to the level structure induced by the applied magnetic field. The m-wavepacket recursion times are also well defined. We turn off the pulsed magnetic field at a time when the wavepacket reaches the high-m turning point, trapping the wavepacket at high l, high m. This coherently transfers Rydberg population to high l, high m, avoiding the incoherent 'diffusion' of Rydberg population equally over all l and m, and could thereby yield lifetime enhancements much greater than n^2.

For the purposes of illustrating the coherent control scheme for enhancement of Rydberg lifetimes, we consider a hydrogenic system with principal quantum number n about 70 evolving in time-dependent crossed electric and magnetic fields (Ivanov & Stolow 1997), as shown in figure 9. The system experiences a pulsed electric field (60 ns FWHM, max. 1 V cm^{-1}). At $t = 0$, on the falling edge of the pulse, a laser prepares a Stark wavepacket at $n = 70$. This leads to a fast evolution in $\langle l \rangle$, as can be seen by the sharp increase (over 0–5 ns) of the solid line of figure 9. The electric field, however, does not vanish, but remains at a residual field of 10 mV cm^{-1}. This causes a further, slow evolution in $\langle l \rangle$, finally reaching the maximum at about 100 ns. Were nothing else to occur, this wavepacket would eventually return again to low l. In order to avoid this, we turn on a pulsed magnetic field (20 ns FWHM, max. 6.5 Gauss) exactly when the Stark wavepacket reaches maximum l (around 100 ns). This causes an evolution in the m quantum numbers, as can be seen by the dashed line in figure 9. In the case shown, the Zeeman wavepacket oscillates twice before the magnetic pulse turns off, leaving the Rydberg state in high m. M_{total} ($= m_{\text{Ry}} + m_{\text{core}}$) is conserved due to the applied cylindrical symmetry from the residual field and, therefore, for decay to occur, the Rydberg electron can only exchange its m with that of the core. Although the residual field mixes rapidly the available l, l can never be less than m_{Ry} and so the decay of the wavepacket is governed by the decay of m_{Ry}. A prepared Rydberg wavepacket with high M_{total} should exhibit very long lifetimes, limited finally by small perturbations.

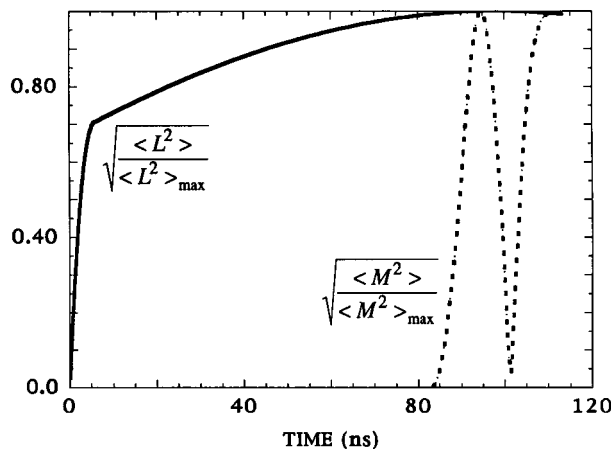In this section, we discussed that fact that ZEKE experiments, even with 'inco-

Figure 9. Use of wavepacket methods to control the lifetimes of Rydberg states, using nanosecond pulsed electric and magnetic fields. A pulsed electric field causes the angular momentum, L, to evolve out to the maximum value at which time a pulsed magnetic field is turned on, causing M to evolve out to the maximum M, at which time the magnetic field turns off. This leaves the Rydberg wavepacket trapped in a high-M state (very long lifetime). For a discussion, see the text.

herent' nanosecond lasers, always prepare Rydberg (Stark) wavepackets due to the enormous density of states at high n. This recognition lead us to suggest that the evolution of these wavepackets can be controlled using time-dependent electric and magnetic fields, in this example to prepare stable circular states.

7. Wavepacket method for isotope separation

We consider the application of wavepacket methods to another practical problem: isotope separation, based upon the preparation (and subsequent extraction) of spatially localized wavepackets.

Traditional methods of isotope separation such as gaseous diffusion and centrifugation rely on slight differences in isotopic mass. Laser isotope separation, on the other hand, relies on small isotope shifts in atomic or molecular spectral lines. It requires both the use of tunable narrowband radiation for selective excitation of one isotope over the others and a detailed knowledge of the spectroscopy of the system. Wavepacket isotope separation (Averbukh *et al.* 1996), by contrast, does *not* rely on spectrally selective excitation. Rather, it makes use of differences between isotopes in their *field-free* wavepacket evolution. For the case of excitation of vibrational wavepackets, the isotopes become separable due to differences in the wavepacket evolution arising from the isotope dependence of vibrational frequencies and anharmonicities. At the point of optimal spatial separation of the wavepackets, one isotope may be selectively extracted (e.g. by ionization) through use of another laser pulse. Wavepackets, however, also delocalize as they evolve. Therefore, the isotope separation scheme must take advantage of the wavepacket revivals. Wavepacket isotope separation combines the advantages of mechanical separation schemes (generality, robustness) with the high single-step enrichment typical of laser separation schemes.

We consider the simple case of a two-component (α and β) isotope mixture of diatomic molecules. A short laser pulse excites the molecules to a higher bound molecular potential, $V_1(R)$. The duration of the excitation pulse is much shorter

than the vibrational periods, T_α and T_β, of both isotopes in the $V_1(R)$ potential, where $T_{\alpha,\beta} = 2\pi/\omega_{\alpha,\beta}$ (and $\omega_{\alpha,\beta}$ are the vibrational frequencies). The isotope shift is defined as $\Delta\omega = |\omega_\alpha - \omega_\beta| \ll \omega_{\alpha,\beta}$. If the vibrational wavepackets in the molecules α and β behaved exactly like classical particles, they would become spatially separated after a time period $t_{\text{sep}} \approx \pi/\Delta\omega$, since at this time the classical vibrational motions of the two wavepackets would be exactly $180°$ out of phase.

For each isotope, a spatially localized vibrational wavepacket is prepared in the upper electronic state by the excitation pulse. No spectral selectivity is used at this stage, and virtually identical wavepackets are excited for both isotopic components. The wavepackets initially undergo periodic oscillatory motion in the V_1 potential. If they were classical particles, then at the time t_{sep} we would simply ionize and extract, for example, the wavepacket at the inner turning point, leaving the other at the outer turning point. However, quantum mechanical dephasing caused by anharmonicity in the molecular potentials leads to a delocalization of the wavepackets after a time $t_{\text{deph}} \approx T_{\text{rev}}/(\Delta n)^2$. (The Δn represents the typical number of vibrational states contained in the wavepacket.) The time t_{deph} is typically much less than t_{sep} and therefore we would not be able to separate the isotopes due to their spatial overlap. Thus, the classical idea of isotope separation fails.

The solution of this problem is to make use of the revival structure of the wavepackets: the classical-like behaviour required for isotope separation recurs periodically. For the case of a Morse oscillator with energy $E(v) = \hbar\omega(v - \kappa v^2)$ and vibrational quantum number v, frequency ω, anharmonicity κ, the revival time is $T_{\text{rev}} = 2\pi/\omega\kappa$.

The best isotope separation is at times when the wavepackets are well localized at a revival and, simultaneously, the wavepacket oscillations of the two isotopes are out of phase by $180°$. This can be seen in figure 10b, where we see wavepacket signals for $^{79}\text{Br}_2$ (shifted up for clarity) and $^{81}\text{Br}_2$: many revivals can be seen. The natural abundance ratio is 1:1. In figure 10a, we show the ratio of the signals from figure 10b over the first few picoseconds of evolution. The wavepackets dephase before they separate and the isotope selectivity is poor. Close inspection of figure 10b reveals that around 32–35 ps, the revivals have become out of phase. The ratio of the isotopes in this region is plotted in figure 10c. Good single shot isotope selectivity is observed and the isotope ratio is seen to vary by 250%: either $^{79}\text{Br}_2$ or $^{81}\text{Br}_2$ may be extracted, depending on the choice of time delay.

In this example, we applied an understanding of wavepackets to the practical problem of isotope separation, demonstrating good single shot selectivity.

8. Wavepacket interferometry

The use of phase-locked pairs of optical pulses can lead to new effects in wavepacket studies: wavepacket interferometry (Scherer *et al.* 1990) (also known as the optical Ramsay effect (Noordham *et al.* 1992)). In the time domain picture, a wavepacket is prepared with a pump pulse. A time delay later, an identical wavepacket is prepared with a identical phase-locked laser pulse. The two wavepackets interfere with each other, leading to either enhancement or destruction of the initial wavepacket, and has therefore been proposed as a method of control. The method has been very successfully applied to controlling excited state population in Cs_2 (Blanchet *et al.* 1995). It has been used to study to excited state non-adiabatic effects in the Ba atom (Schumacher *et al.* 1997). It has also been applied to ultrafast creation and destruction of free carriers in quantum well devices (Heberle *et al.* 1995).
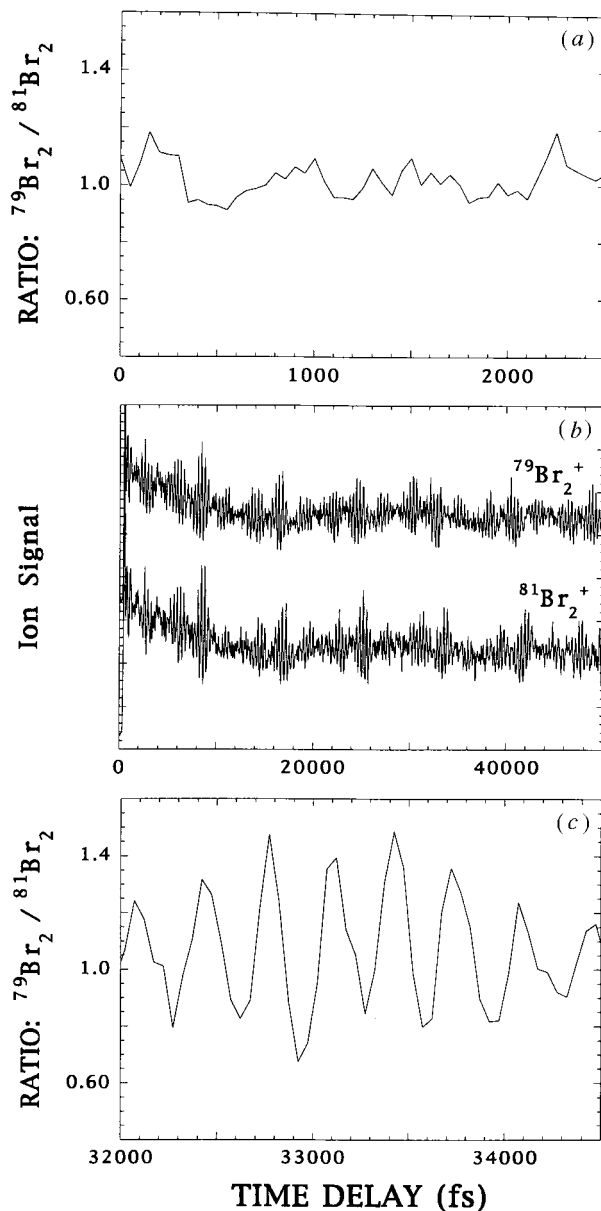
Figure 10. Use of wavepacket methods for isotope separation. In (*b*), a series of revivals for $^{79}Br_2$ and $^{79}Br_2$ are shown. The wavepackets dephase before they can get out of phase, as shown in (*a*). At a characteristic time, the wavepackets are simultaneously 180° out of phase and at a revival, leading to efficient isotope separation (*c*).

There is a simple frequency domain interpretation of such experiments. When an optical pulse is split in two and recombined with a delay, the spectrum of the pulse is altered. This is a linear optical Michelson interferometer: each frequency ω_i in the pulse interferences with itself constructively or destructively, depending on the path difference between the two arms. The net form of these optical interferences can be seen from a consideration of the Fourier power spectrum of the two pulses.

It is a time-domain double slit: the spectrum of two identical pulses separated by a delay Δ contains light and dark fringes whose spacing varies inversely with Δ. As the time delay between the pulses increases, the fringe spacing in the spectrum decreases. When the light fringes overlap with the eigenstates of the quantum system of interest, optical transitions are observed. When the dark fringes overlap the eigenstates of the quantum system, no optical transitions are observed. As always, modification of the spectrum (e.g. tuning the laser frequency) has a large effect on the excited state population.

This simple frequency domain interpretation does not mean, however, that the method should be disregarded. For example, in the case of multiphoton transitions (Jones 1995; Blanchet *et al.* 1997), the frequency domain interpretation is less straight forward. However, even in the single photon case, these experiments provide a new means to manipulate optical properties of materials on a timescale faster than the natural response time of the material itself. Consider interacting with the quantum system (as prepared with two phase locked pulses), using a third laser pulse, on the timescale of $t' = \Delta$, for example, in between the two phase locked pulses. This means that optical properties of the material system (e.g. carrier density, refractive index, etc.), as experienced by the third pulse, may be manipulated on the timescale of Δ. (In other words, the full fringe spectrum of the pulse pair will not develop due to the truncation of the Fourier integral at time t'.) This timescale can be much faster than the natural response time of the material, which is set by the inverse linewidths of the optical transition. This phenomenon was noted in studies of carrier control in quantum wells (Heberle *et al.* 1995). Hence, this potentially provides a new method of ultrafast switching, at up to THz frequencies, of a third laser.

9. Conclusion

In this paper we have considered the application of wavepacket methods to a variety of problems. Wavepackets are well understood in terms of their creation, free evolution and detection. Wavepackets have been used for time domain spectroscopy and give a very useful classical-like picture of the ultrafast evolution of zero-order states (for example, Zewail 1994; Manz & Wöste 1995). We described some wavepacket phenomenology of bound states (i.e. revival structure) and questioned the proposition that wavepacket methods be considered as a new 'technology' to be applied to the solution of other problems.

We discussed the isomorphism between coherent control experiments and traditional femtosecond pump-probe experiments. The latter are very successful examples of control in a broad range of systems. Wavepackets are usually thought to probe effects on the femtosecond timescale. However, the first example we gave of wavepacket applications was the study of microsecond timescale effects in Rydberg states. A careful analysis of ion versus ZEKE femtosecond wavepacket detection lead to the observation of ion–Rydberg interactions (l mixing) which occur on a microsecond timescale. The next example was recognizing that the Rydberg states prepared by conventional 'incoherent' nanosecond lasers in typical ZEKE experiments are in fact wavepackets, due to the extremely high density of electronic states exceeding the coherence bandwidth of these lasers. Recognizing this fact allowed for the design of a pulsed electric and magnetic field scheme to control the Rydberg population through coherent l and m mixing. The target in this scheme was to prepare a high-l high-m wavepacket which should be very stable against delay. The third example we gave

in this paper was the application of wavepackets to isotope separation. Through an understanding of wavepacket revival structure and its dependence on isotopic mass, we were able to demonstrate a general isotope separation scheme based upon the phase shifting of the revivals at long time delays. In the final section, we discussed wavepacket interferometry, based upon the creation and subsequent interference of identical wavepackets. Although this method has a simple frequency domain interpretation and will not lead to new spectroscopic observations, it may have an important role to play in manipulating optical properties of materials on timescales faster than the natural response of the material itself (Heberle *et al.* 1995). This may lead to new kinds of ultrafast (THz) switches.

These simple examples are meant not to be real examples of new technologies. Rather, they are modestly meant to illustrate that wavepackets can be thought of as a tool, applied under the appropriate circumstances, to be used to study or modify other kinds of problems. There is an on-going revolution in short pulse laser technology. Whenever a technology makes such advances, we should look carefully at its implications. The efforts of many groups on the creation and controlled shaping of short optical pulses (for example, Wefers *et al.* 1995; Melinger *et al.* 1994; Kohler *et al.* 1995; Bardeen *et al.* 1995; Schumacher *et al.* 1995) provide powerful tools for wavepacket control. It remains a question perhaps worthy of investigation whether or not these advances in wavepacket methods will have a broader impact in science and technology.

References

Averbukh, I. S. & Perel'man, N. F. 1991 *Sov. Phys. Usp.* **34**, 572.

Averbukh, I. S., Vrakking, M. J. J., Villeneuve, D. M. & Stolow, A. 1996 *Phys. Rev. Lett.* **77**, 3518.

Banin, U., Waldman, A. & Ruhman, S. 1992 *J. Chem. Phys.* **96**, 2416.

Baranov, L. Y., Remacle, F. & Levine, R. D. 1996 *Phys. Rev.* A **54**, 4789.

Barbara, P. F., Knox, W. H., Mourou, G. A. & Zewail, A. H. 1994 *Ultrafast phenomena IX.* Berlin: Springer.

Bardeen, C. J., Wang, Q. & Shank, C. V. 1995 *Phys. Rev. Lett.* **75**, 3410.

Baumert, T., Engel, V., Röttgermann, C., Strunz, W. T. & Gerber, G. 1992 *Chem. Phys. Lett.* **191**, 639.

Bixon, M. & Jortner, J. 1996 *Mol. Phys.* **89**, 373.

Blanchet, V., Aziz-Bouchene, M. & Girard, B. 1995 *Chem. Phys. Lett.* **233**, 491.

Blanchet, V., Nicole, C., Bouchene, M.-A. & Girard, B. 1997 *Phys. Rev. Lett.* **78**, 2716.

Brumer, P. & Shapiro, M. 1989 *Accts. Chem. Res.* **22**, 407.

Brumer, P. & Shapiro, M. 1992 *A. Rev. Phys. Chem.* **34**, 257.

Chupka, W. A. 1993 *J. Chem. Phys.* **98**, 4520.

Dantus, M., Janssen, M. H. M. & Zewail, A. H. 1991 *Chem. Phys. Lett.* **181**, 281.

de Vivie Riedle, R., Kobe, K., Manz, J., Meyer, W., Reischl, B., Rutz, S., Schreiber, E. & Wöste, L. 1996 *J. Phys. Chem.* **100**, 7789.

Fischer, I., Villeneuve, D. M., Vrakking, M. J. J. & Stolow, A. 1995 *J. Chem. Phys.* **102**, 5566.

Fischer, I., Vrakking, M. J. J., Villeneuve, D. M. & Stolow, A. 1996 *Chem. Phys.* **207**, 331.

Gordon, R. J. & Rice, S. A. 1998 *A. Rev. Phys. Chem.* (In the press.)

Gruebele, M. & Zewail, A. H. 1993 *J. Chem. Phys.* **98**, 883.

Gruebele, M., Roberts, G., Dantus, M., Bowman, R. M. & Zewail, A. H. 1990 *Chem. Phys. Lett.* **166**, 459.

Heberle, A. P., Baumberg, J. J. & Kohler, K. 1995 *Phys. Rev. Lett.* **75**, 2598.

Ivanov, M. Y. & Stolow, A. 1997 *Chem. Phys. Lett.* **265**, 231.

Jones, R. R. 1995 *Phys. Rev. Lett.* **75**, 1491.

Kohler, B., Yakovlev, V. V., Che, J., Krause, J. L., Messina, M., Wilson, K. R., Schewenter, N., Whitnell, R. M. & Yan, Y. J. 1995 *Phys. Rev. Lett.* **74**, 3360.

Kosloff, R., Rice, S. A., Gaspard, P., Tersigni, S. & Tannor, D. J. 1989 *Chem. Phys.* **139**, 201.

Krause, K. J., Messina, M., Wilson, K. R. & Yan, Y. J. 1995 *J. Phys. Chem.* **99**, 13 763.

Manz, J. & Wöste, L. (eds) 1995 *Femtosecond chemistry.* New York: VCH.

Marmet, L., Held, H., Raithel, G., Yeazell, J. A. & Walther, H. 1994 *Phys. Rev. Lett.* **72**, 3779.

Meacher, D. R., Meyler, P. E., Hughes, I. G. & Ewart, P. 1991 *J. Phys.* B **24**, L63.

Melinger, J. S., Gandhi, S. R., Hariharan, A., Goswami, D. & Warren, W. S. 1994 *J. Chem. Phys.* **101**, 6439.

Merkt, F. & Zare, R. N. 1995 *J. Chem. Phys.* **101**, 3495.

Müller-Dethlefs, K. & Schlag, E. W. 1991 *A. Rev. Phys. Chem.* **42**, 109.

Müller-Dethlefs, K., Sander, M. & Schlag, E. W. 1984 *Z. Naturforsch.* A **39**, 1089.

Nauenberg, M., Stroud Jr, C. R. & Yeazell, J. 1994 *Sci. Amer.* **270**, 24.

Noordham, L. D., Duncan, D. I. & Gallagher, T. F. 1992 *Phys. Rev.* A **45**, 4734.

Park, S. M., Lu, S.-P. & Gordon, R. J. 1991 *J. Chem. Phys.* **94**, 8622.

Pierce, A. P., Dahleh, M. A. & Rabitz, H. 1990 *Phys. Rev.* A **42**, 1065.

Pugliano, N., Szarka, A. Z., Palit, D. K. & Hochstrasser, R. M. 1993 *J. Chem. Phys.* **99**, 7273.

Remacle, F. & Levine, R. D. 1996 *J. Chem. Phys.* **105**, 4649.

Rodriguez, G., John, P. C. & Eden, J. G. 1995 *J. Chem. Phys.* **103**, 10 473.

Rose, T. S., Rosker, M. J. & Zewail, A. H. 1988*a J. Chem. Phys.* **88**, 6672.

Rose, T. S., Rosker, M. J. & Zewail, A. H. 1988*b Chem. Phys. Lett.* **146**, 175.

Rose, T. S., Rosker, M. J. & Zewail, A. H. 1989 *J. Chem. Phys.* **91**, 7415.

Scherer, N. F., Ruggiero, A. J., Du, M. & Fleming, G. R. 1990 *J. Chem. Phys.* **93**, 856.

Schumacher, D. W., Hoogenraad, J. H., Pinkos, D. & Bucksbaum, P. H. 1995 *Phys. Rev.* A **52**, 4719.

Schumacher, D. W., Lyons, B. J. & Gallagher, T. F. 1997 *Phys. Rev. Lett.* **78**, 4359.

Shi, S., Woody, A. & Rabitz, H. 1988 *J. Chem. Phys.* **88**, 6870.

Tannor, D. J. & Rice, S. A. 1988 *Adv. Chem. Phys.* **70**, 441.

Villeneuve, D. M., Fischer, I. & Stolow, A. 1995 *Opt. Commun.* **114**, 141.

Vrakking, M. J. J. & Lee, Y. T. 1995 *J. Chem. Phys.* **102**, 8818.

Vrakking, M. J. J., Villeneuve, D. M. & Stolow, A. 1996*a J. Chem. Phys.* **105**, 5647.

Vrakking, M. J. J., Villeneuve, D. M. & Stolow, A. 1996*b Phys. Rev.* A **54**, R37.

Vrakking, M. J. J., Fischer, I., Villeneuve, D. M. & Stolow, A. 1995 *J. Chem. Phys.* **103**, 4538.

Wals, J., Fielding, H., Christian, J., Snoek, L., van der Zande, W. & van Linden van den Heuvell, H. B. 1994 *Phys. Rev. Lett.* **72**, 3783.

Wang, X., Bersohn, R., Takahashi, K., Kawasaki, M. & Kim, H. L. 1996 *J. Chem. Phys.* **105**, 2992.

Wang, Q., Schoenlein, R. W., Peteanu, L. A., Mathies, R. A. & Shank, C. V. 1994 *Science* **266**, 422.

Wefers, M. M., Kawashima, H. & Nelson, K. A. 1995 *J. Chem. Phys.* **102**, 9133.

Williams, R. M., Papanikolas, J. M., Rathje, J. & Leone, S. R. 1996 *Chem. Phys. Lett.* **261**, 405.

Yan, Y. J., Gillian, R. E., Whitnell, R. M., Wilson, K. R. & Mukamel, S. 1993 *J. Chem. Phys.* **97**, 2320.

Yeazell, J. A. & Stroud, C. R. 1991 *Phys. Rev.* A **43**, 5153.

Yeazell, J. A., Mallalieu, M. & Stroud, C. R. 1990 *Phys. Rev. Lett.* **64**, 2007.

Zewail, A. H. 1994 *Femtosecond chemistry.* Singapore: World Scientific.